# Driving-Style-Based Co-Design Optimization of an Automated Electric Vehicle: A Cyber-Physical System Approach

Chen Lv, *Member, IEEE,* Xiaosong Hu, *Senior Member, IEEE,* Alberto Sangiovanni-Vincentelli, *Fellow, IEEE,* Yutong Li, Clara Marina Martinez, and Dongpu Cao, *Member, IEEE*

***Abstract*—This paper studies the co-design optimization approach to determine how to optimally adapt automatic control of an intelligent electric vehicle to driving styles. A cyber-physical system (CPS) based framework is proposed for co-design optimization of the plant and controller parameters for an automated electric vehicle, in view of vehicle's dynamic performance, drivability, and energy along with different driving styles. System description, requirements, constraints, optimization objectives and methodology are investigated. Driving style recognition algorithm is developed using unsupervised machine learning and validated via vehicle experiments. Adaptive control algorithms are designed for three driving styles with different protocol selections. Performance exploration method is presented. Parameter optimizations are implemented based on the defined objective functions. Test results show that an automated vehicle with optimized plant and controller can perform its tasks well under aggressive, moderate, and conservative driving styles, further improving the overall performance. The results validate the feasibility and effectiveness of the proposed CPS-based co-design optimization approach.**

***Index Terms*— Co-design optimization, Automated electric vehicle, Driving style, Cyber-physical systems.**

## I. Introduction

AUTOMATED vehicles have been gaining increasing attention from both academia and industrial sectors [1]. The field of intelligent vehicles exhibits a multidisciplinary nature, involving transportation, automotive engineering, information, energy and security [2]-[5]. Intelligent vehicles have increased their capabilities in highly and even fully automated driving. However, unresolved problems do exist due to strong uncertainties and complex driver-vehicle interactions.

Chen Lv is with the School of Mechanical and Aerospace Engineering and the School of Electrical and Electronic Engineering, Nanyang Technological University, Singapore (e-mail: henrylvchen@gmail.com).

Xiaosong Hu is with the Department of Automotive Engineering and the State Key Lab of Mechanical Transmission, Chongqing University, Chongqing 400044, China, and the Advanced Vehicle Engineering Centre, Cranfield University, Bedford MK43 0AL, UK (e-mail: xiaosonghu@ieee.org).

Alberto Sangiovanni-Vincentelli is with the Department of Electrical Engineering and Computer Sciences, University of California, Berkeley, Berkeley, California 94720, USA (e-mail: alberto@berkeley.edu).

Yutong Li is with the College of Transportation Engineering, Tongji University, Shanghai, China. (e-mail: wilson420813@gmail.com).

Clara Marina Martinez is with Porsche Engineering R&D Center, Germany. (e-mail: c.m.marina@cranfield.ac.uk).

Dongpu Cao is with Mechanical and Mechatronics Engineering, University of Waterloo, ON, N2L 3G1, Canada (e-mail: dongpu.ca@gmail.com) (Corresponding authors are Dongpu Cao and Xiaosong Hu)

### A. Driver-Vehicle Interactions

Highly automated vehicles are likely to be on public roads within a few years. Before transitioning to fully autonomous driving, driver behavior should be better understood and integrated to enhance vehicle performance and traffic efficiency [6]-[9]. To address these challenges, researchers have explored advanced driver assistance systems (ADAS), and human-machine interface (HMI) from a variety of points of view [10], [11]. However, since the dynamic relationships between driver and vehicle are highly complex, satisfactory driver-vehicle interactions should go beyond the present ADAS and HMI systems. Human-vehicle interactions have already being considered in a high-level closed loop, where driving style, driving feel and vehicle performance, are considered [12]. Driving style plays a very important role in vehicle energy efficiency and ride comfort, thus significantly impacting controller synthesis [12]-[14]. For instance, control objectives and control protocols should be adaptively adjusted according to different driving styles. Based on the findings reported in [13], a better understanding of driving styles could help improve ADAS performance and further reduce vehicle's fuel consumption through driver feedback. In [14], an enhanced intelligent driver model was developed, and then it was used to investigate the impact of different driving strategies on traffic capacity. In [15], an adaptive cruise control strategy considering the characteristics of different driving styles was developed, and the proposed strategy could automatically adapt to different traffic situations. Nevertheless, advanced control and optimization of vehicle systems with characterized driving styles are still open challenges and worthwhile exploring.

### B. Automated Electrified Vehicles

The ever-growing attention to the environment and energy conservation requires automobiles to be cleaner and more efficient [16]-[18]. In this study, an electric vehicle (EV) is chosen as the platform to conduct our research in automated driving. Based on existing studies, small changes in driving style can cause unnecessary energy waste and sub-optimal performance of an EV [19], [20]. Moreover, regenerative braking capability of EVs can be enhanced by prior knowledge

of driving style. Hence, an optimal energy management strategy can be obtained with knowledge about the entire driving cycle, environment, and driver behaviors. Therefore, the information of operating scenarios, driver behaviors and driver-vehicle interactions is crucial and should be integrated to enhance the energy efficiency of automated electric vehicles.

### C. Cyber-Physical Systems Approach

A Cyber-Physical System (CPS) is a distributed, networked system that fuses computational processes (cyber world) with the physical world [21], [22]. An EV is a typical example of CPS. In details, an automated EV involves the following subsystems: the controller, representing the "Cyber" world, the physical plant, the "Human" driver, and the environment. These different elements, which are highly coupled, decide the vehicle's behavior and overall performance, as Fig. 1 shows.

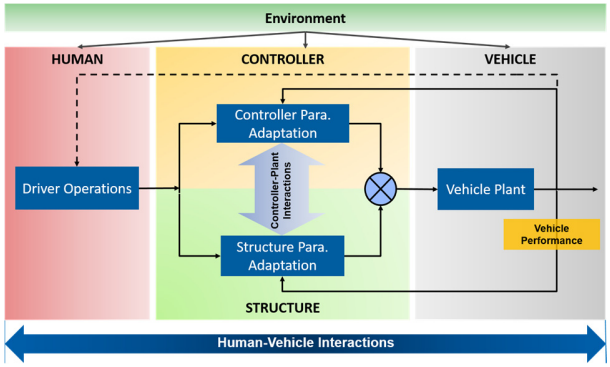


Fig. 1. CPS based human-vehicle interactions.

The main issue of the existing approaches in vehicle design and control is the lack of global optimality in the selection of system architecture, physical parameters, and control variables [23]. In this context, the emerging co-design method provides the capability to extend system design space and further enhance the performance of CPS [24]-[28]. In [24], a platform-based design method utilizing contracts to do the high-level abstraction of the components in a CPS was proposed, and it is able to offer support to the overall design process. In [26], co-design optimization of a cyber physical vehicle system, which considers task time, actuator characteristics, energy consumption and processor workload, was investigated. In [27], a CPS-based control framework was developed for vehicle systems to minimize the car-following fuel consumption and ensure inter-vehicle safety. Besides the cyber and the physical worlds, we also need to take "Human" of an automated vehicle into consideration. Thus, the interactive impacts between the vehicle plant, control variables, multi-performance and driver styles, should be well understood.

To further advance the existing CPS methods as well as their applications reported in [29-31], following contributions are made in this paper: 1) a CPS-based co-design optimization framework is proposed for an automated EV considering different driving styles; 2) a driving style recognition algorithm is developed using unsupervised learning method; 3) control algorithms are synthesized for typical driving styles with different protocol selections.

The rest of the paper is organized as follows: The co-design optimization problem is formulated in Section II. System models with experimental validation are presented in Section III. Section IV presents the vehicle controller synthesis for three driving styles with different control protocol selections. Then, the performance exploration method is presented in Section V. Section VI reports test results of design optimization, followed by conclusions presented in Section VII.

## II. Problem Formulation

In this section, the co-design of an automated electric vehicle with different driving styles is formulated as a multi-objective optimization problem. The goal is to find optimal assignments for design variables to maximize performances while satisfying a number of constraints. To ensure the problem to be solved within a reasonable complexity, the following assumptions are made: 1) The vehicle operates in normal conditions, and vehicle stability could be guaranteed by stability control functions; 2) Only longitudinal motion control is considered in this study; 3) The sizing of the electric powertrain is fixed, i.e., the parameters of the battery and the electric motor are constant to bound the exploration space.

### A. Hierarchical Optimization Methodology

The optimization problem is formulated as a constrained multi-objective one where both vehicle and controller parameters need to be chosen. In this paper, the Platform-Based Design (PBD) is adopted as the co-design methodology [21].

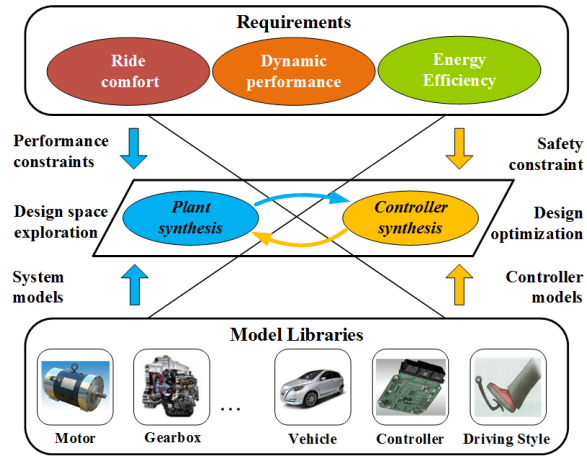


Fig. 2. Platform-Based design optimization of the electric vehicle.

As Fig. 2 shows, PBD is a meet-in-the-middle approach that favors re-usability. At the top layer, there are high-level requirements and constraints. The bottom layer is defined by a design *platform*, i.e., a library of components characterized by their behaviors and performance. In this paper, the bottom layer contains the models of the vehicle, electric powertrain, brakes, and driver-style-based controller. The models are parametrized to capture families of the system, components and controllers. The design problem is to select a set of components and their parameters so that the constraints are satisfied with the objective functions optimized. The selection process is called mapping, indicated as the middle-layer meeting point in the diagram, since the obligations captured in the requirements and constraints are discharged by particular components or

combinations thereof. Co-design of the physical parameters, controller protocols and variables, for the intelligent electric vehicle is then made possible.

### B. System Description

*1) Physical plant:* For the structure of the studied automated electric vehicle, a central electric motor is installed at the front axle of the vehicle. During acceleration, the motor, which is powered by the battery, provides propulsion through the transmission system to the wheels. During deceleration, the regenerative braking torque generated by the motor is blended with the friction braking modulated by the hydraulic modulator.

*2) Control architecture:* The high-level strategy for the longitudinal motion control of the automated EV is designed to track a reference acceleration, generated via the pre-defined acceleration profile, as shown in Fig. 3. The reference acceleration profile is a 3D look-up table defined by the reference vehicle speed $v_{ref}$, the ego-vehicle speed $v$, and the reference acceleration $a_{ref}$.

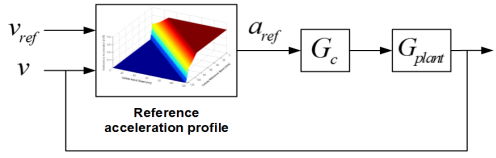


Fig. 3. Longitudinal motion control architecture of the intelligent vehicle.

### C. Driving Event

A *driving event* is a driving maneuver, such as acceleration, deceleration, turning, and lane change, which can be used to identify driving styles [28]. As mentioned above, this paper mainly focuses on longitudinal motion control, hence the adopted driving events are defined as [29]:

*1) Event 1: 0-50km/h acceleration*. In this event, the car is accelerated from 0 to 50 km/h. The vehicle acceleration, jerk, and the time taken in this process are typical performance indices. This event is used to optimize and evaluate the dynamic performance and ride comfort under different driving styles.

*2) Event 2: 50-0 km/h deceleration*. In this event, the car is decelerated from 50 km/h to 0. The deceleration and the time taken in this process are typical performance indices. The energy recovered during the braking process can be used to evaluate energy efficiency. This event is used to optimize and check vehicle's dynamic performance and energy efficiency under different driving styles.

*3) Event 3: driving cycle.* Although the energy consumption of the vehicle can be evaluated in the above two events, the time duration of an acceleration or deceleration procedure is relatively short, making it difficult to evaluate energy consumption at the vehicle level. Thus, the ECE driving cycle is adopted for measuring energy efficiency under different driving styles. The ECE driving cycle, which is a series of data points representing the vehicle speed versus time, exhibits the typical driving conditions of a car in urban areas [17]. It is usually adopted to carry out road testing for studying the fuel economy of a passenger car.

### D. Driving Style Recognition

To identify driving style for control synthesis and system optimization, a driving style recognition (DSR) algorithm is developed using unsupervised machine learning with partially labelled data. The data set is collected in the road tests with a Sedan-Type vehicle, and it is comprised of 9 real life cycles covering over 500 km. The data can be overall classified into three groups according to the driver feedback as aggressive, conservative and moderate. These three driving styles are firstly defined as [29]-[34]:

*1) Aggressive:* Aggressive drivers exhibit frequent changes in throttle and brake pedal positions [32]. They drive with sharp and abrupt accelerations and decelerations, aiming at vehicle dynamic performance. This kind of behavior would result in higher fuel consumption and increased likelihood of accidents [29].

*2) Conservative:* Conservative drivers often exhibit mild operational behaviors with small amplitudes and low-frequency actions on steering wheel, accelerator and brake pedal [33]. They value energy efficiency and ride comfort, and avoid abrupt variations of vehicle state.

*3) Moderate:* Moderate drivers are positioned between the above two. They would like to balance multiple performances, such as vehicle dynamic performance, ride comfort, and energy efficiency [29].

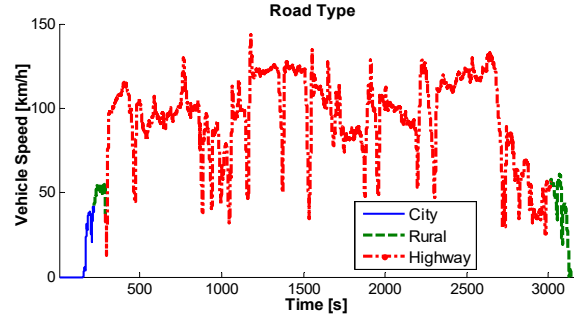


Fig. 4. The real life route used for DSR experimental validation.

The unlabelled data set is pre-processed for driving events detection and statistics extraction. A total amount of six signals is used: throttle pedal position, brake light switch, longitudinal and lateral accelerations, steering wheel angle and vehicle speed. Five statistics are extracted per event: maximum, minimum, mean, standard deviation and root mean square. The reduced set of signals is clustered using Gaussian Mixture Models (GMM), which generates the DSR classification algorithm to be implemented onboard. The performance of the DSR algorithm is validated against the subjective labels and further tested with a new set of data from a new real life route with changeable road type, as shown in Fig. 4. This new data set is collected by a SUV-type vehicle with a different driver.

TABLE I. DRIVING STYLE RECOGNITION RESULTS IN SUV CYCLES

| | Agg. Cycles | Moderate Cycle | Conserv. Cycle |
|---|---|---|---|
| Acceleration | 0.55 (*149*) | 0.43 (*113*) | 0.34 (*106*) |
| Brake | 0.58 (*33*) | 0.56 (*25*) | 0.36 (*22*) |
| Cruise | 0.83 (*149*) | 0.69 (*126*) | 0.70 (*124*) |
| Turn | 0.41 (*6*) | 0.29 (*7*) | 0.29 (*7*) |

Table I shows the results of the SUV driving data using the

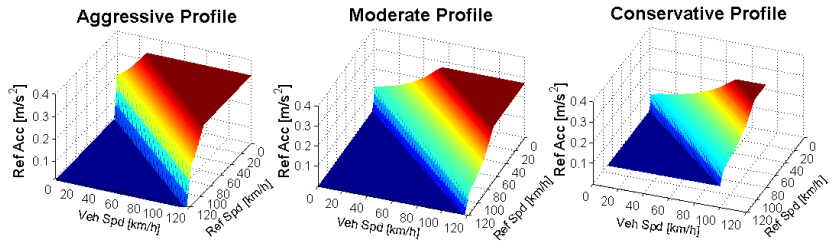


Fig. 5. Pre-defined 3D reference acceleration profiles.

developed DSR algorithm. So as to quantitatively evaluate the performance of the algorithm, the driving cycles are classified per events using the aggressiveness index. The aggressiveness index is transformed from the classification into an equivalent index, assigning an increasing value from 0 to 1 to the different events based on the level of aggressiveness [34]. To provide further information about the robustness of each classification, the number of events identified is included in brackets and italics. According to the results, the conservative cycle is classified as the least aggressive one, particularly by acceleration and brake events analysis. The moderate cycle is situated between the aggressive and conservative ones. While the aggressive cycle is identified as the sportiest one, but it has a similar braking level with the moderate one, agreeing with driver's feedback. Finally, the consistency and robustness of the algorithm are verified using the test data set. The test shows consistency in the identification and aligns with drivers' perception. The above testing results validate the suitability of this approach for DSR, its onboard implement capability and robustness to vehicle and driver characteristics. More detailed algorithms with experimental results can be found in [34].

Based on the above recognition and classification algorithms, the features of aggressive, conservative and moderate driving styles can be extracted, and online recognition of a driver's driving style can be realized using the well-trained model as well. Meanwhile, according to the above features obtained, the 3 dimensional human-like acceleration profiles are developed for each driving style, as illustrated in Fig. 5.

### E. Requirements for Vehicle Design and Optimization

The requirements for vehicle design and control involve dynamical performance, energy efficiency, and ride comfort. Driving style consideration implies the introduction of multiple trade-offs between performances that are set as the objective functions in our optimization problem, under different driving styles, operating conditions, and driving tasks.

*1) Dynamic performance:* Dynamic performance is considered as the fundamental and the most important indicator of a car [29]. Maximum speed and acceleration time are proxies for dynamic performance. In this paper, we select the 0-50 km/h acceleration time $t_{acc}$ and the 50-0 km/h deceleration time $t_{brk}$ as two indicators for the dynamic performance to capture driver's behavior and select suitable value for the gear ratio $i_g$.

*2) Ride comfort:* The comfort level of a vehicle, also known as drivability, can be assessed by vehicle's jerk $j$, which is the second derivative of the vehicle's longitudinal velocity $v$ [17]:

$$j = \ddot{v} \tag{1}$$

During acceleration, torsional oscillations may occur in the drivetrain due to fast torque transitions, resulting in unexpected jerks at vehicle level and deteriorated drivability. To cope with this problem, an active damping controller is usually required [36]. Although aggressive drivers may enjoy fierce acceleration and jerk, for those who prefer conservative or moderate driving style, ride comfort is a very important performance. In this paper, jerk is used to capture the comfort level of the vehicle.

*3) Energy efficiency:* The energy efficiency of a vehicle can be represented by the energy consumed during a certain trip. Typically, energy consumption can be reduced by optimizing the powertrain energy management [29]. For electrified vehicles, it can be further enhanced through regenerative braking. Thus, in this paper, the regenerated braking energy defined in equation (2) is set as one of the optimization goals in the trade-off problem [18].

$$E_{reg} = \eta_{gen} \cdot \int T_{m,reg}\omega_m dt \tag{2}$$

where $E_{reg}$ is the regenerated braking energy, $T_{m,reg}$ and $\omega_m$ are the regenerative braking torque and the angular speed of the electric motor, respectively, and $\eta_{gen}$ is the generation efficiency of the motor.

### F. Constraints for Vehicle Design and Optimization

Constraints in the optimization problem involve indicators that are set to stay within specific bounds to limit the search space.

*1) Maximum vehicle speed:* The constraint on vehicle speed is posed as:

$$v_{\max} = r\pi n_{\max} / (30 i_g) \geq (100/3.6)\, m/s \tag{3}$$

where $v_{\max}$ is the maximum speed of the vehicle, $n_{\max}$ is the highest rotational speed of the electric motor, $r$ is the nominal radius of tire, and $i_g$ is the gear ratio.

*2) Minimum gradeability: Gradeability* is defined as the highest grade that a vehicle can achieve with a maintained speed. Once the motor parameters are given, this performance is determined by the gear ratio, as equation (4) shows [35].

$$\eta_t i_g T_{m,\max} = mgr(f\cos\alpha_{\max} + \sin\alpha_{\max}) \tag{4}$$

$$i_{\max} = \tan\alpha_{\max} \geq 30\% \tag{5}$$

where $T_{m,\max}$ is motor's peak torque, $m$ is the total mass of the vehicle, $\eta_t$ is the efficiency of the transmission system, $f$ is the friction drag coefficient, and $\alpha$ is the grade angle.

*3) Minimum brake intensity:* In order to guarantee stability during braking, a vehicle needs to have enough braking force, represented by the brake intensity $z$, as required by regulation ECE-R13 [36]:

$$z = \dot{v}/g \geq 0.1 + 0.85(\varphi - 0.2) \tag{6}$$

where $\varphi$ is the adhesion coefficient of the road.

*4) Powertrain limits:* According to the assumption described above, the characteristics of the power source are given, then the limitation on motor torque can be described by:

$$T_m \omega_m \le P_{m,lim} \tag{7}$$

where $T_m$ is output torque of the electric motor, and $P_{m,lim}$ is the peak power of the electric motor.

## III. System Modelling and Validation

### A. Electric Powertrain system

The electric powertrain is comprised of an electric motor, a gearbox, a final drive, a differential, and half shafts. The motor torque is modelled as a first-order reaction, as shown in equation (8). The models for the drivetrain dynamics and half-shaft torque can be given by equation (9) and (10) [25].

$$T_{m,ref} = T_m + \tau_m \dot{T}_m \tag{8}$$

$$J_m \ddot{\theta}_m = T_m - 2T_{hs} / i_g \tag{9}$$

$$T_{hs} = k_{hs}(\theta_m / i_g - \theta_w) + c_{hs}(\dot{\theta}_m / i_g - \dot{\theta}_w) \tag{10}$$

where $\tau_m$ is the small time constant, $T_{m,ref}$ is the reference torque of the electric motor, $T_{hs}$ is the half-shaft torque, $J_m$ is the motor inertia, and $\theta_m$ and $\theta_w$ are the angular positions of electric motor and load, respectively. $k_{hs}$ and $c_{hs}$ are the stiffness and damping coefficients of the half shaft, respectively.

In this paper, the battery is built as an open-circuit voltage-resistance model. Look-up tables are compiled on the basis of the state of charge (SOC) and temperature data of the battery, modeling its charging-discharging internal resistance. The detailed model with parameters can be found in [17].

### B. Blended brake system

The brake force distribution (BFD) should adhere to the ideal curve. To simplify the implementation and to avoid real-time modulation of brake pressure, the BFD is usually set as a fixed value, which is determined by the parameters of the installed brake devices, as shown in Fig. 6(a). The front and rear braking demands can be calculated as follows [17]:

$$T_b = 2T_{b,fw} + 2T_{b,rw} \tag{11}$$

$$T_{b,fw} = \beta T_{b,dmd} / 2 \tag{12}$$

$$T_{b,rw} = (1-\beta) T_{b,dmd} / 2 \tag{13}$$

where $T_b$ is the actual braking torque provided by the blended brakes, $T_{b,dmd}$ is the demanded braking torque of the vehicle, and $T_{b,fw}$ and $T_{b,rw}$ are the requested braking torque of one front wheel and one rear wheel, respectively. $\beta$ is the BFD ratio.

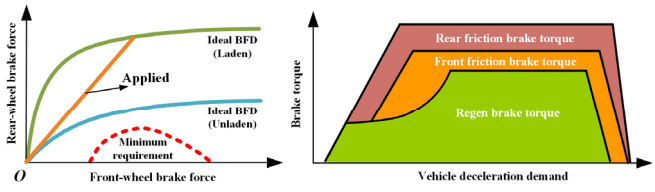


Fig. 6. Brake force distribution strategy.

As shown in Fig. 6(b), during deceleration, the overall demanded braking torque of the vehicle is supplied by the regenerative and the friction blending braking. The overall braking torque is controlled to be consistent with driver's deceleration intention. The reference values for the regenerative and frictional braking on front axle can be given by:

$$T_{m,reg} = \min(2T_{b,fw} / i_g, T_{m,reg,lim}) \tag{14}$$

$$T_{b,fw,fric} = T_{b,fw} - 2T_{m,reg} / i_g \tag{15}$$

where $T_{m,reg}$ and $T_{m,reg,lim}$ are reference torque and torque limit of the regenerative braking of the electric motor, respectively. $T_{b,fw,fric}$ is the frictional braking torque of the front wheel.

### C. Dynamic model of the vehicle and tyre

A model of vehicle dynamics with seven degrees of freedom has been built. The tyre model, which is of great importance for research on acceleration and deceleration, should be able to simulate the real tyre in both adhesion and sliding. In this article, the well-known Pacejka magic formula tyre model is adopted [37]. The detailed models were described in [17].

### D. Experimental validation

The models of the electric vehicle with its subsystems were implemented in MATLAB/Simulink. Experimental data measured from vehicle test were used for model calibration. Key parameters of the systems are listed in Table II. The feasibility and effectiveness of the models have been previously validated via hardware-in-the-loop experiments and vehicle road testing [17, 25].

TABLE II. Key Parameters of the Electric Vehicle.

| Parameter | Value | Unit |
|---|---|---|
| Vehicle mass | 1360 | kg |
| Wheel base | 2.50 | m |
| Frontal area | 2.40 | $m^2$ |
| Gear ratio | 7.881 | — |
| Nominal radius of tyre | 0.295 | m |
| Coefficient of air resistance | 0.32 | — |
| Motor peak power | 45 | kW |
| Motor maximum torque | 145 | Nm |
| Motor maximum speed | 9000 | rpm |
| Battery voltage | 336 | V |
| Battery capacity | 66 | Ah |

## IV. Controller Design For Different Driving Styles

### A. High-Level Controller Architecture

The high-level supervisory controller adopts a scheduling protocol, asking the architecture and control objectives of the low-level controller, as well as the parameters of the physical plant, to dynamically adapt to different driving styles, as shown in Fig. 7. In this study, the driving style of the automated vehicle can be either obtained in the manual mode through the DSR algorithm developed in Section II, or actively selected by human operator during autonomous mode. To avoid unexpected discontinuities in controller output resulted by frequent and fast transitions between different driving styles, a simple and reliable approach for the application is to allow the driving style to be actively or passively switched only when the vehicle is stopped, i.e. the vehicle speed $v$=0.

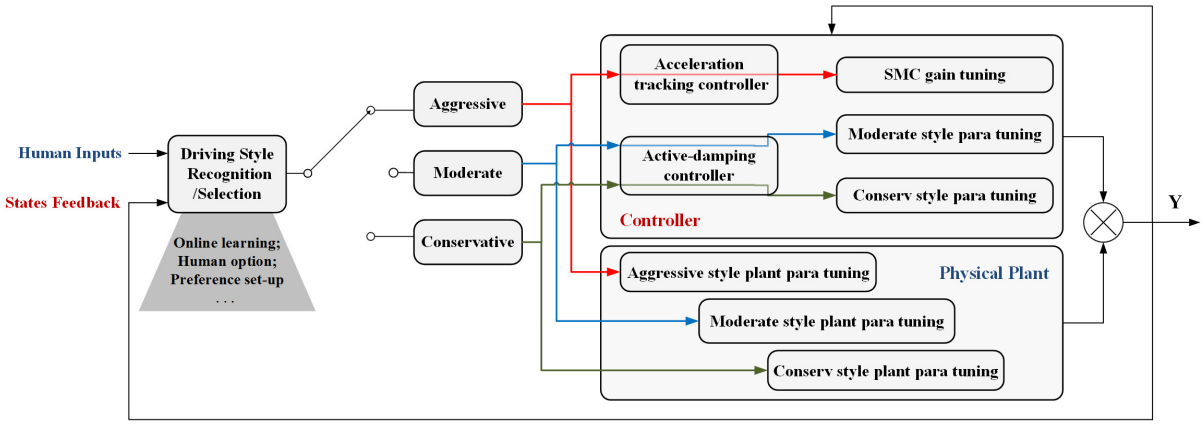


Fig. 7. Scheduling-protocol based hierarchical control for different driving styles.

### B. Low-Level Controller for different driving styles

*1) Controller for aggressive driving style:* Based on the sporty feature of aggressive driving style, the vehicle longitudinal control under this condition can be seen as an acceleration tracking problem, realizing the sporty feel in automated driving for passengers. Because of its ability to address nonlinearity and achieve good performance with fast response [38], a sliding-mode control (SMC) scheme is applied.

In designing the sliding-mode controller, the error term is defined as:

$$e = a - a_{ref} \tag{16}$$

where $a$ and $a_{ref}$ are the actual and reference values of vehicle acceleration, respectively.

To guarantee zero steady error, an integral-type sliding surface $S$ is chosen as:

$$S = \int e dt \tag{17}$$

One method for designing a control law that derives the system trajectories to the sliding surface is the Lyapunov direct method. The following Lyapunov function is used:

$$V = \frac{1}{2} SS \tag{18}$$

To ensure the stability of the system, the derivative of the Lyapunov function should satisfy the following condition:

$$\dot{V} = S\dot{S} \le 0 \tag{19}$$

Thus, if $\dot{S} = 0$, the above stability condition can be satisfied.

For the purpose of controller design, a control-oriented longitudinal vehicle model without considering wheel slip is used [35].

$$a = \frac{1}{mr} i_g T_m - fg - \frac{1}{2m} C_D A \rho v^2 \tag{20}$$

where $r$ is the nominal radius, $C_D$ is the coefficient of air resistance, $A$ is the frontal area, and $\rho$ is the air density, $f$ is the friction drag coefficient, and $g$ is the gravitational acceleration.

Then, substituting equations (16) and (20) into equation (17), when $\dot{S} = 0$, the SMC control law can be derived as:

$$T_{m,ref} = \frac{mr}{i_g}\left( a_{ref} + fg + \frac{C_D A \rho v^2}{2m} - k_{SMC}\,\mathrm{sgn}(S) \right) \tag{21}$$

where $k_{SMC}$ is the positive gain of the SMC controller, and sgn($S$) is the sign function defined as:

$$\mathrm{sgn}(S) = \begin{cases} 1, & S > 0 \\ 0, & S = 0 \\ -1, & S < 0 \end{cases} \tag{22}$$

**Remark 1**. It is well known that in the standard SMC, the discontinuous sign function, sgn($S$), may cause chattering when the state trajectories are approaching the sliding surfaces. To avoid this phenomenon, the discontinuous term in equation (21) could be replaced by a continuous function $S$, removing the chatter from the control input [39], as shown in equation (23).

$$T_{m,ref} = \frac{mr}{i_g}\left( a_{ref} + fg + \frac{C_D A \rho v^2}{2m} - k_{SMC} S \right) \tag{23}$$

*2) Controller for moderate driving style:* The moderate driving style features a balanced performance in vehicle dynamics and ride comfort. To this end, the low-level plant controller uses a combined feed-forward and feed-back structure, to actively damp powertrain torsional vibrations, thus mitigating the longitudinal jerk and enhancing drivability:

$$T_{m,ref} = T_{ff} + T_{fb} \tag{24}$$

where $T_{ff}$ is the feed-forward input term required for tracking and $T_{fb}$ is the feedback component designed to reduce the control error.

Based on the control objective, the feed-forward term can be determined by the target motor torque $T_{m,tgt}$, which is calculated using the reference acceleration:

$$T_{ff} = T_{m,tgt} \tag{25}$$

For the feedback term, a linear proportional-integral (PI) controller is adopted to damp the torsional oscillation:

$$T_{fb} = (K_P + K_I \int dt) \cdot e' \tag{26}$$

$$e' = T_{m,tgt} - 2T_{hs} / i_0 i_g \tag{27}$$

where the feedback gains $K_P$ and $K_I$ are tuning parameters of the *PI* controller, and $e'$ is the tracking error.

*3) Controller for conservative driving style:* Since the conservative drivers usually care more about energy efficiency and smooth driving feel by carefully operating the brake and acceleration pedals, the low-level plant controller adopts the same combined feed-forward and feed-back architecture as the moderate one to ensure vehicle drivability.

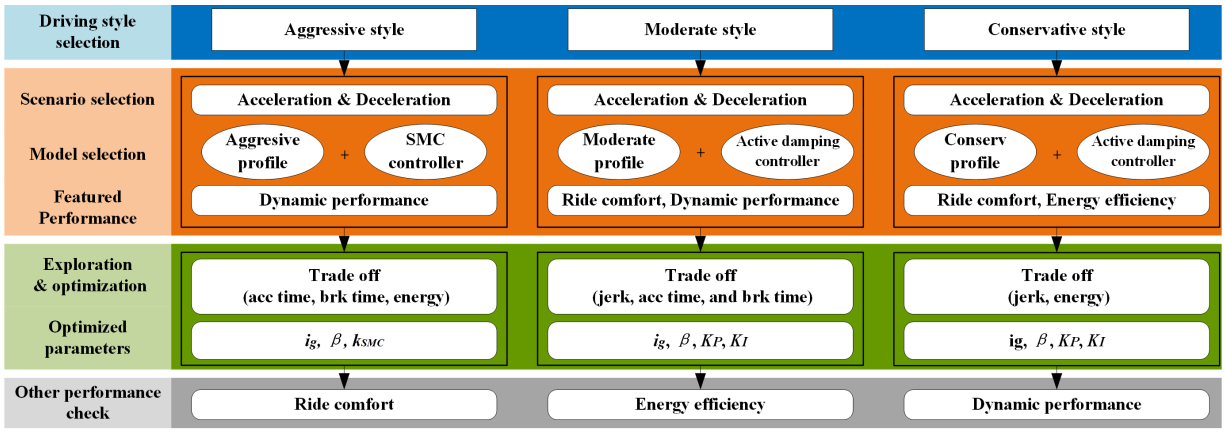


Fig. 8. The proposed co-design optimization flow for the vehicle with three driving styles.

## V. Driving-Style-Based Performance Exploration and Parameter Optimization

### A. Design Space Exploration

Based on the system constrains formulated in Section II, namely the requirements for vehicle speed, grade-ability, and brake stability shown in equation (3)-(6), the boundaries of the related physical plant parameters can be calculated, and the design space is then achieved.

### B. Performance Exploration Methodology

In order to carry out multi-objective optimization under different driving styles, the impacts of related parameters on the performance indicators should be explored. To do so, thefollowing exploration algorithm is proposed.

TABLE III. Algorithm For Performance Exploration.

**Algorithm 1: Performance Exploration**
**Input:** Parameter Library $\{P_1,\ldots,P_i,C_1,\ldots,C_j\} \subseteq \xi$, Event $E$
**Output:** Best Performance Point $K$
**function** Global Exploration ($\xi$, $E$)
*Performance* ← {}; *Paras* ← {};
**while** $p_1 \in P_1$ **do**
**while** $p_2 \in P_2$ **do**
⋮
**while** $p_i \in P_i$ **do**
**while** $c_1 \in C_1$ **do**
**while** $c_2 \in C_2$ **do**
⋮
**while** $c_j \in C_j$ **do**
*Performance* ← Simulation ($E$,$P_1$,..,$P_i$,$C_1$,..,$C_j$)
**end while**
Paras ← Performance ($C_j$);
⋮
**end while**
Paras ← Performance ($C_1$,$C_2$,…,$C_j$);
**end while**
Paras ← Performance ($P_i$, $C_1$,$C_2$,…,$C_j$);
⋮
**end while**
Paras ← Performance($P_1$, $P_2$,…,$P_i$, $C_1$,$C_2$,…,$C_j$);
K ← Best Performance Point (Paras);
**Return K, Paras**
**end function**

As shown in Table III, assuming that, within the Parameter Library $\xi$, there are several parameters, namely $P_1$, $P_2$,…,$P_i$, $C_1$, $C_2$,…,$C_j$, deciding one *Performance*. $P_1$, $P_2$,…,$P_i$ represent parameters of the physical plant, while $C_1$, $C_2$,…,$C_j$ indicate controller variables. Under pre-defined driving event $E$ with valid design space, the selected vehicle *Performance* is simulated in the Simulink environment stepping each parameter with a suitably small step. After simulation-based global exploration, the *Best Performance K* with its corresponding value selections of the parameters can be attained.

### C. Driving-Style-Oriented Multi-Objective Optimization

*1) Aggressive-driving-style based optimization:* This driving style requires to maximize vehicle dynamic performance first and foremost. However, a good performance in terms of energy efficiency is also expected to be guaranteed. Therefore, the trade-off between dynamic performance and energy efficiency is considered, with a much greater weight on the side of dynamic performance.

$$\{i_g, k_{SMC}, \beta\} = \arg\min_{-E_{reg}} \left(\omega_1 \cdot t_{acc} + \omega_2 \cdot t_{brk} + \omega_3 \cdot j - \omega_4 \cdot E_{reg}\right) \quad (28)$$

*2) Moderate-driving-style based optimization:* In this case, the multi-objective optimization problem is set as a trade-off between dynamic performance and ride comfort:

$$\{i_g, K_P, K_I, \beta\} = \arg\min_{j} \left(\omega_1 \cdot t_{acc} + \omega_2 \cdot t_{brk} + \omega_3 \cdot j - \omega_4 \cdot E_{reg}\right) \quad (29)$$

*3) Conservative-driving-style based optimization:* As mentioned before, under the conservative driving style, the drivers' behavior is usually mild with intentions of saving energy and ensuring comfort. Thus, in this mode, the trade-off elements are switched to ride comfort and energy efficiency:

$$\{i_g, K_P, K_I, \beta\} = \arg\min_{-E_{reg}} \left(\omega_1 \cdot t_{acc} + \omega_2 \cdot t_{brk} + \omega_3 \cdot j - \omega_4 \cdot E_{reg}\right) \quad (30)$$

For weighting selection, a much greater value would be put on the side of each featured performance under different driving styles, and the weight on non-considered performance is set as zero. The difference of the weights between featured and sub-featured performances are set to be an order of magnitude. The detailed set-up for the weightings under different driving styles is summarized in Table IV. The overall optimization flow and procedure are shown in Fig. 8.

TABLE IV. Weight Selection for Different Styles

| Driving Style | Weights | | | |
|---|---|---|---|---|
| | $\omega_1$ | $\omega_2$ | $\omega_3$ | $\omega_4$ |
| Aggressive | 10 | 10 | 0 | 1 |
| Moderate | 10 | 0 | 10 | 1 |
| Conservative | 0 | 0 | 1 | 1 |

## VI. Optimization Results and Analysis

Based on the proposed co-design method, the performance exploration and system optimization are carried out in MATLAB/Simulink. The simulations are implemented iteratively with developed models under defined driving events at each operating point (i.e. each selected value of plant and control parameters) for the three driving styles, generating multiple performances. The detailed results with each driving style are reported as follows.

### A. Optimization results for the aggressive driving style

Since the optimization problem under the aggressive driving style is formulated as a trade-off between vehicle dynamic performance and energy efficiency with a much greater weight on the side of dynamic performance, during optimization the interactive effects of the values of the SMC gain, the gear ratio, and BFD on the dynamic performance of 0-50km/h acceleration and regenerated braking energy are explored.

According to the exploration results shown in the subplots (a) and (b) of Fig. 9, the positive gain $K$ of the SMC controller tends to be small, while the gear ratio prefers a larger value in favor of a better acceleration performance. For the regenerative braking performance, the variation of the gear ratio barely affects the overall regenerated energy, although BFD needs to select a smaller value to reach a higher efficiency according to the exploration results. This is due to the fact that more braking torque demand will be distributed to the front axle, which is the driven axle, indicating a larger proportion taken up by the regenerative braking among the overall braking torque.

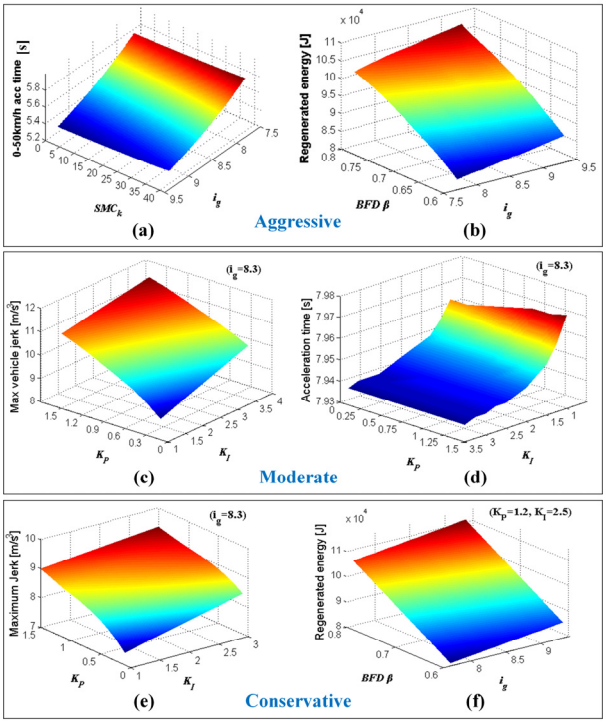


Fig. 9. Performance exploration results of the three driving style.

### B. Optimization results of the moderate driving style

Based on the multiple optimization objectives under the moderate driving style, the trade-off between ride comfort and acceleration performance is considered. Taking the exploration scenario under a fixed value of the gear ratio at 8.3 as an example, and according to the results shown in the subplots (c) and (d) of Fig. 9, the selection of the gains in the linear PI controller for active damping has a great impact on the control performance of the vehicle jerk. With selection of $K_P$ and $K_I$ at 1.5 and 3.0, respectively, the maximum vehicle jerk during a 50-0 km/h deceleration process is over 10.0 m/s$^3$. While setting the two parameters to 0.5 and 2.0, the maximum jerk can be reduced to about 8.0 m/s$^3$, improving ride comfort effectively. However, the manipulation of the gains of the active damping controller has small influence on the acceleration performance, according to the exploration results. The detailed optimization results for parameter selection are summarized in Table V.

### C. Optimization results of the conservative driving style

Since the controller structure of the conservative style is quite similar to the moderate one, the related parameters to be optimized ($K_P$, $K_I$, $i_g$, and $\beta$) are the same. However, because the optimization objectives are different under these two styles, the values of the parameters at the end of the optimization process can be far different, as the subplots (e) and (f) of Fig. 9 show.

### D. Comparison and discussion

A comparison of the above results is shown in Fig. 10. The aggressive style, which favors dynamic performance, dominates the acceleration and deceleration events among the three. The duration of the events of 0-50km/h acceleration and 50-0km/h deceleration under aggressive driving are 5.36 s and 4.16 s, respectively. The conservative style, which is in favor of ride comfort and energy efficiency, achieves the best performance in vibration reduction and regenerative braking. The maximum jerk under conservative driving is below 7 m/s$^3$, which is around 1/3 of that in the aggressive driving. Finally, the moderate style, which sits in between the other two, achieves a good balance between dynamic performance, ride comfort, and energy efficiency.

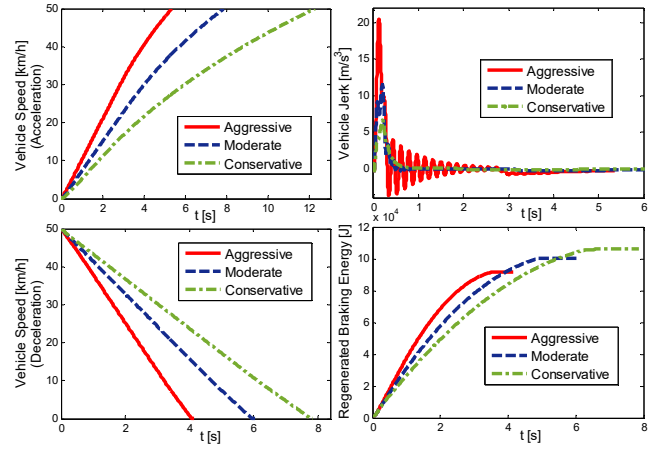


Fig. 10. Optimized results for the vehicle under different driving styles.

To compare the energy efficiency at the vehicle level with designed control protocols and parameter selections during different driving styles, the standard ECE driving cycle is used. According to the test data in Table VI, the energy consumption of the automated electric vehicle under the conservative style is

575.9 kJ, which improves the efficiency by over 10%, compared to the energy used in aggressive driving.

TABLE V. OPTIMIZED PERFORMANCE UNDER DIFFERENT DRIVING STYLES

| Driving Style | | Performance | | | | |
|---|---|---|---|---|---|---|
| | | $t_{acc}$ /s | $t_{brk}$ /s | $j_{max}$ /m/s$^3$ | $E_{reg}$ /$10^4 J$ | $E_{ECE}$ /$10^4 J$ |
| Aggress | CPS based | 5.36 | 4.16 | 20.47 | 9.17 | 64.06 |
| | wo CPS | 5.71 | 4.35 | 19.21 | 9.42 | 63.21 |
| Moderate | CPS based | 7.88 | 6.04 | 11.52 | 10.04 | 60.19 |
| | wo CPS | 9.26 | 6.35 | 11.91 | 9.49 | 62.06 |
| Conserv | CPS based | 12.27 | 7.86 | 6.69 | 10.60 | 57.59 |
| | wo CPS | 13.56 | 8.28 | 10.13 | 9.35 | 59.21 |

Additionally, a comparison of the results between the CPS based optimization and the baseline is performed. According to the data listed in Table VI, the vehicle with CPS based optimization achieves better comprehensive performances in vehicle dynamics, ride comfort, and energy efficiency, thanks to the co-design of the plant and controller parameters. This demonstrates the advantages of the newly proposed method over the conventional one.

## VII. CONCLUSIONS

In this paper, a CPS-based framework for co-design optimization of an automated electric vehicle with different driving styles was proposed. The multi-objective optimization problem was formulated. The driving style recognition algorithm was developed using unsupervised machine learning and validated via vehicle testing. The system modelling and experimental verification were carried out. Vehicle control algorithms were synthesized for three typical driving styles with different protocol selections. The performance exploration methodology and algorithms were proposed. Test results show that the overall performances of the vehicle were significantly improved by the proposed co-design optimization approach. Future work will be focused on real vehicle application of the proposed methods and CPS design methodology improvement.

## ACKNOWLEDGMENT

The research was supported in part by the Young Elite Scientist Sponsorship Program by CAST (No. 2017QNRC001) and the EU-funded Marie Sklodowska-Curie Individual Fellowships (IF) Project under Grant 706253-pPHEV-H2020-MSCA-IF-2015.

## REFERENCES

[1] Petrovskaya, A. and Thrun, S. "Model based vehicle detection and tracking for autonomous urban driving." Autonomous Robots 26, no. 2-3 (2009): 123-139.

[2] González, D., Pérez, J., et al. A review of motion planning techniques for automated vehicles. IEEE Transactions on Intelligent Transportation Systems, 2016, 17(4), pp.1135-1145.

[3] Shi, Y., Qin, J. and Ahn, H.S. "Distributed Coordination Control and Industrial Applications." IEEE Transactions on Industrial Electronics 64, no. 6 (2017): 4967-4971.

[4] C. Lv, D. Cao, et al., "Analysis of autopilot disengagements occurring during autonomous vehicle testing," IEEE/CAA Journal of Automatica Sinica, vol. 5, pp. 58-68, 2018.

[5] Shen, C., Shi, Y. and Buckham, B. "Integrated path planning and tracking control of an AUV: A unified receding horizon optimization approach." IEEE/ASME Transactions on Mechatronics 22, no. 3 (2017): 1163-1173.

[6] C. Lv, H. Wang, D. Cao, Y. Zhao, D. J. Auger, M. Sullman, et al., "Characterization of Driver Neuromuscular Dynamics for Human-Automation Collaboration Design of Automated Vehicles," IEEE/ASME Transactions on Mechatronics, 2018, in press.

[7] X. Ji, Y. Liu, et al., "Interactive Control Paradigm based Robust Lateral Stability Controller Design for Autonomous Automobile Path Tracking with Uncertain Disturbance: A Dynamic Game Approach," IEEE Transactions on Vehicular Technology, 2018, in press.

[8] Li, H., Shi, Y. and Yan, W. "Distributed receding horizon control of constrained nonlinear vehicle formations with guaranteed γ-gain stability." Automatica 68 (2016): 148-154.

[9] W. Zhao, X. Qin, and C. Wang, "Yaw and lateral stability control of Automotive four-wheel steer-by-wire system," IEEE/ASME Transactions on Mechatronics, 2018, in press.

[10] D. I. Katzourakis, D. A. Abbink, et al, "Steering Force Feedback for Human-Machine-Interface Automotive Experiments," IEEE Transactions on Instrumentation and Measurement, vol. 60, pp. 32-43, 2011.

[11] F. Miedl and T. Tille, "3-D Surface-Integrated Touch-Sensor System for Automotive HMI Applications," IEEE/ASME Transactions on Mechatronics, vol. 21, pp. 787-794, 2016.

[12] N. R. Kapania and J. C. Gerdes, "Design of a feedback-feedforward steering controller for accurate path tracking and stability at the limits of handling," Vehicle System Dynamics, vol. 53, pp. 1687-1704, 2015.

[13] R. Wang and S. Lukic, "Review of driving conditions prediction and driving style recognition based control algorithms for hybrid electric vehicles", Vehicle Power and Propulsion Converence, pp. 1-7, 2011.

[14] A. Kesting, M. Treiber, and D. Helbing, "Enhanced intelligent driver model to access the impact of driving strategies on traffic capacity," Philosophical Transactions of the Royal Society of London A: Mathematical, Physical and Engineering Sciences, vol. 368, pp. 4585-4605, 2010.

[15] A. Kesting, M. Treiber, M. Schönhof, and D. Helbing, "Extending Adaptive Cruise Control to Adaptive Driving Strategies," Transportation Research Record: Journal of the Transportation Research Board, vol. 2000, pp. 16-24, 2007.

[16] C. Lv, Y. Xing, t al., "Hybrid-Learning-Based Classification and Quantitative Inference of Driver Braking Intensity of an Electrified Vehicle," IEEE Transactions on Vehicular Technology, 2018, in press.

[17] J. Zhang, C. Lv, J. Gou, and D. Kong, "Cooperative control of regenerative braking and hydraulic braking of an electrified passenger car," Proceedings of the Institution of Mechanical Engineers, Part D: Journal of Automobile Engineering, vol. 226, pp. 1289-1302, 2012.

[18] W. Zhao, H. Zhang, and Y. Li, "Displacement and force coupling control design for automotive active front steering system," Mechanical Systems and Signal Processing, vol. 106, pp. 76-93, 2018..

[19] J. Neubauer and E. Wood, "Accounting for the variation of driver aggression in the simulation of conventional and advanced vehicles," SAE Technical Paper, No. 2013-01-1453, 2013.

[20] L. Li, S. You, C. Yang, B. Yan, J. Song, and Z. Chen, "Driving-behavior-aware stochastic model predictive control for plug-in hybrid electric buses," Applied Energy, 2016, 162, 868-897.

[21] P. Derler, E. A. Lee, et al, "Modeling Cyber-Physical Systems," Proceedings of the IEEE, vol. 100, no. 1, pp. 13 - 28, Jan. 2012.

[22] A. Sangiovanni-Vincentelli, W. Damm, and R. Passerone, "Taming dr. frankenstein: Contract-based design for cyber-physical systems," European journal of control, vol. 18, pp. 217-238, 2012.

[23] C. Lv, Y. Xing, et al., "Levenberg-Marquardt Backpropagation Training of Multilayer Neural Networks for State Estimation of A Safety Critical Cyber-Physical System," IEEE Transactions on Industrial Informatics, 2017, in press.

[24] P. Nuzzo, A. Sangiovanni-Vincentelli, et al, "A Platform-Based Design Methodology with Contracts and Related Tools for the Design of Cyber-Physical Systems," Proc. IEEE, vol. 103, no. 11, pp. 2104- 2132, 2015.

[25] C. Lv, Y. Liu, et al, "Simultaneous Observation of Hybrid States for Cyber-Physical Systems: A Case Study of Electric Vehicle Powertrain," IEEE Transactions on Cybernetics, 2018, in press.

[26] Bradley, J.M. and Atkins, E.M. Cyber-Physical Optimization for Unmanned Aircraft Systems. Journal of Aerospace Information Systems, 11(1), pp.48-60, 2014.

[27] Hu, X., Wang, H. and Tang, X. "Cyber-Physical Control for Energy-Saving Vehicle Following with Connectivity." IEEE Transactions on Industrial Electronics, 2017.

[28] Y. Li, C. Lv, et al, "High-Precision Modulation of A Safety-Critical Cyber-Physical System: Control Synthesis and Experimental Validation," IEEE/ASME Transactions on Mechatronics, 2018, in press.
[29] Lv, C., Wang, H., et al. Cyber-Physical System Based Optimization Framework for Intelligent Powertrain Control. SAE International Journal of Commercial Vehicles, 2017, 10, pp.254-264.
[30] Finn, J., Nuzzo, P. and Sangiovanni-Vincentelli, A. "A mixed discrete-continuous optimization scheme for cyber-physical system architecture exploration." In Proceedings of the IEEE/ACM International Conference on Computer-Aided Design, pp. 216-223. IEEE Press, 2015.
[31] Lv, C., Zhang, J., Nuzzo, P., Sangiovanni-Vincentelli, A., et al. "Design optimization of the control system for the powertrain of an electric vehicle: A cyber-physical system approach." In Mechatronics and Automation, IEEE International Conference on, pp. 814-819. IEEE, 2015.
[32] E. Gilman, A. Keskinarkaus, S. Tamminen, et al, "Personalised assistance for fuel-efficient driving," Transportation Research Part C: Emerging Technologies, vol. 58, pp. 681-705, 2015.
[33] Martinez, C.M., Heucke, M., Wang, F.Y., et al. "Driving style recognition for intelligent vehicle control and advanced driver assistance: A survey." IEEE Transactions on Intelligent Transportation Systems, 2017.
[34] C. M. Martínez, "iHorizon-Enabled Energy Management for Plug-in Hybrid Electric Vehicles", Ph.D. dissertation, Dept. Auto. Eng., Cranfield University, Bedford, UK, 2017.
[35] M. Mitschke, H. Wallentowitz, Dynamik der Kraftfahrzeuge, 4th ed., Springer Verlag, Berlin, 2004.
[36] Y. Gao, M. Ehsani, Electronic braking system of EV and HEV - Integration of regenerative braking, automatic braking force control and ABS. No. 2001-01-2478, SAE Technical Paper, 2001.
[37] H.B. Pacejka, E. Bakker. The magic formula tyre model. Vehicle system dynamics, 21(S1), 1-18, 1992.
[38] B. Song, J.K. Hedrick, Dynamic surface control of uncertain nonlinear systems: An LMI Approach, Springer, 2011.
[39] A. Fazeli, M. Zeinali and A. Khajepour, Application of adaptive sliding mode control for regenerative braking torque control. IEEE/ASME Transactions on Mechatronics, vol. 17, pp. 745-755, 2012.

**Chen Lv** (S'14-M'16) is an Assistant Professor of School of Mechanical and Aerospace Engineering and School of Electrical and Electronic Engineering, Nanyang Technological University, Singapore. He received the Ph.D. degree at Department of Automotive Engineering, Tsinghua University, China in 2016. He was a Research Fellow at Advanced Vehicle Engineering Center, Cranfield University, UK during 2016 and 2018, and a joint PhD researcher at EECS Dept., University of California, Berkeley, USA during 2014 and 2015. His research focuses on cyber-physical systems, advanced vehicle control and intelligence, where he has contributed over 60 papers and obtained 11 granted China patents.

Dr. Lv serves as a Guest Editor for IEEE/ASME Transactions on Mechatronics and IEEE Transactions on Industrial Informatics, and an Associate Editor for International Journal of Electric and Hybrid Vehicles, and International Journal of Vehicle Systems Modelling and Testing. He received the Highly Commended Paper Award of IMechE UK in 2012, the NSK Outstanding Mechanical Engineering Paper Award in 2014, the China SAE Outstanding Paper Award in 2015, the 1st Class Award of China Automotive Industry Scientific and Technological Invention in 2015, and the Tsinghua University Outstanding Doctoral Thesis Award in 2016.

**Xiaosong Hu** (SM'16) received the Ph.D. degree in Automotive Engineering from Beijing Institute of Technology, China, in 2012.

He did scientific research and completed the Ph.D. dissertation in Automotive Research Center at the University of Michigan, Ann Arbor, USA, between 2010 and 2012. He is currently a professor at the State Key Laboratory of Mechanical Transmissions and at the Department of Automotive Engineering, Chongqing University, Chongqing, China. He was a postdoctoral researcher at the Department of Civil and Environmental Engineering, University of California, Berkeley, USA, between 2014 and 2015, as well as at the Swedish Hybrid Vehicle Center and the Department of Signals and Systems at Chalmers University of Technology, Gothenburg, Sweden, between 2012 and 2014. He was also a visiting postdoctoral researcher in the Institute for Dynamic systems and Control at Swiss Federal Institute of Technology (ETH), Zurich, Switzerland, in 2014. His research interests include modeling and control of alternative powertrains and energy storage systems.

Dr. Hu has been a recipient of several prestigious awards/honors, including Emerging Sustainability Leaders Award in 2016, EU Marie Currie Fellowship in 2015, ASME DSCD Energy Systems Best Paper Award in 2015, and Beijing Best Ph.D. Dissertation Award in 2013.

**Alberto Sangiovanni-Vincentelli** holds the Buttner Chair of Electrical Engineering and Computer Sciences, at the University of California, Berkeley, where he has been on the faculty since 1976. He helped founding Cadence and Synopsys, the two leading companies in EDA. He is on the Board of Directors of Cadence, Sonics, Expert Systems, and Cogisen. He is a member of the Investment Committee of Atlante Venture, of the Advisory Board of Innogest, Walden International and Xseed, and of the Executive Committee of the Italian Institute of Technology. He was the President of the Strategic Committee of the Italian Strategic Fund. He consulted for companies such as Intel, HP, Bell Labs, IBM, Samsung, UTC, Kawasaki Steel, Fujitsu, Telecom Italia, Pirelli, GM, BMW, Mercedes, Magneti Marelli, ST Microelectronics, ELT, Unipol and UniCredit. He earned the IEEE/RSE Maxwell Award for "groundbreaking contributions that have had an exceptional impact on the development of electronics and electrical engineering", the Kaufmann Award for seminal contributions to EDA, the EDAA lifetime Achievement Award, the IEEE/ACM R. Newton Impact Award, the University of California Distinguished Teaching Award, and the IEEE Graduate Teaching Award for inspirational teaching of graduate students. He is an ACM fellow, a member of the National Academy of Engineering and holds two honorary Doctorates. He authored over 850 papers, 17 books and 2 patents.

**Yutong Li** is currently a Postdoc in Department of Transportation at Tongji University. He received his B. Eng. (2012) from the Jilin University, and his Ph.D. (2017) from Tsinghua University. His research interests broadly include topics in Decision making and control under uncertainties (application to autonomous vehicles), Simulation based verification and validation, Powertrain architecture optimization for performance and fuel economy. He received Tsinghua first class scholarship for doctoral student in 2013 and 2015, and the China SAE Outstanding Paper Award in 2015.

**Clara Marina Martinez** received her Ph.D. degree at Advance Vehicle Engineering Centre, Cranfield University, UK, in 2017. She obtained the 5-years degree in Industrial Engineering from Seville University, Spain, and the MSc degree in automotive mechatronics from Cranfield University in 2014. She is currently with Porsche Engineering R&D Center, Germany. Her current research focuses on intelligent control for electrified vehicles, driving style recognition, future speed prediction, and machine learning. She has published over 10 papers.

**Dongpu Cao** (M'13) received the Ph.D. degree from Concordia University, Canada, in 2008. He is currently an Associate Professor at Mechanical and Mechatronics Engineering, University of Waterloo, Canada. His research focuses on vehicle dynamics and control, automated driving and parallel driving, where he has contributed more than 100 publications and 1 US patent. He received the ASME AVTT'2010 Best Paper Award and 2012 SAE Arch T. Colwell Merit Award. Dr. Cao serves as an Associate Editor for IEEE TRANSACTIONS ON INTELLIGENT TRANSPORTATION SYSTEMS, IEEE TRANSACTIONS ON VEHICULAR TECHNOLOGY, IEEE TRANSACTIONS ON INDUSTRIAL ELECTRONICS, IEEE/ASME TRANSACTIONS ON MECHATRONICS and ASME JOURNAL OF DYNAMIC SYSTEMS, MEASUREMENT, AND CONTROL. He has been a Guest Editor for VEHICLE SYSTEM DYNAMICS, and IEEE TRANSACTIONS ON HUMAN-MACHINE SYSTEMS. He serves on the SAE International Vehicle Dynamics Standards Committee and a few ASME, SAE, IEEE technical committees.